

## Diurnal Evolution of Three-Dimensional Wind and Temperature Structure in California's Central Valley

SHIYUAN ZHONG

*Department of Geosciences, University of Houston, Houston, Texas*

C. DAVID WHITEMAN

*Pacific Northwest National Laboratory, Richland, Washington*

XINDI BIAN

*U.S. Department of Agriculture Forest Service North Central Research Station, East Lansing, Michigan*

(Manuscript received 28 January 2004, in final form 21 May 2004)

### ABSTRACT

The diurnal evolution of the three-dimensional summer-season mean wind and temperature structure in California's Sacramento and San Joaquin Valleys (collectively called the Central Valley) is investigated using data from 22 radar wind profiler/radio acoustic sounding systems (RASS) operated as part of the Central California Ozone Study in 2000. The profiler network revealed, for the first time, that the persistent summer-season flow pattern documented by surface observations extends 800–1000 m above the surface. At most locations, up-valley winds persist during both day and night except at the upper ends of the valleys and close to the valley sidewalls where diurnal wind reversals occur. Wind speeds exhibit pronounced diurnal oscillations, with amplitudes decreasing with height. A low-level wind maximum occurs in the lowest 300 m, with a sharp decrease in speed above the maximum. Especially well defined nocturnal low-level jets occur at sites in the southern San Joaquin Valley, where maximum speeds of  $10 \text{ m s}^{-1}$  or more occur 1–2 h before midnight at heights near 300 m. The afternoon mixed layer, generally deeper than 1000 m, increases in depth with up-valley distance in both valleys. At night, temperature inversions develop in the lowest several hundred meters with near-isothermal layers above. Mean temperatures in the lowest 500 m of the valleys are always warmer than at the same altitude over the coast, and temperature increases from the lower to upper valleys. The diurnal oscillations of the coast-valley and along-valley temperature and pressure difference reach a maximum in late afternoon and a minimum in early morning. These oscillations are in phase with the diurnal variation of westerly onshore flows. The along-valley wind maxima, however, occur 1–2 h before midnight, whereas the along-valley pressure gradient maxima are usually found just before sunset.

### 1. Introduction

The evolution of boundary layer wind and temperature structure is an important factor governing the spatial distribution and temporal variation of air pollutants for any given region. The lack of spatial and temporal resolution in standard upper-air observations often leads to an inadequate description of the three-dimensional wind and temperature structure and its diurnal variations, especially in areas of complex terrain where synoptic-scale flows can be greatly modified by topography and mesoscale or local thermal forcing, confounding air-

quality forecasting. Central California is a region in which, because of ocean-land contrasts, complicated mountain massifs of variable heights, and a summertime climatological regime favoring weak synoptic-scale flows, local winds are often dominated by thermal forcing and are poorly understood because of a lack of adequate upper-air observations.

Low-level winds in central California have been the subject of several previous observational studies (Hays et al. 1984). These studies typically used data from the standard network of surface and upper-air observations. Frenzel (1962) carried out a comprehensive study of diurnal wind variations in central California using data from 21 surface weather stations and 3 four-times-per-day upper-air sounding sites for July of 1958. Using hodographs of 1-month-averaged winds at each station, he showed for the San Francisco Bay area that land-

---

*Corresponding author address:* Dr. Sharon Zhong, Department of Geosciences, University of Houston, 312 S & R 1, 4800 Calhoun Rd., Houston, TX 77204-5007.  
E-mail: szhong@uh.edu

water contrasts are most significant to the airflow and that air motion in the interior Sacramento and San Joaquin Valleys (collectively called the Central Valley) reflects, in part, channeling by the high Sierra Nevada ridgeline to the east. The general flow pattern is a westerly flow at the coast, which enters the Central Valley at the Carquinez Strait and is then diverted northward and southward into the Sacramento and San Joaquin Valleys; it is upon this flow that diurnal circulations are superimposed.

Using hourly wind observations from four double-theodolite pilot balloon stations surrounding the Central Valley city of Sacramento on three days in the summer of 1972 as part of an urban meteorology study, Myrup et al. (1983) examined the three-dimensional structure of the wind field near Sacramento. Although the local topography is relatively uniform, the analyses revealed a complex wind field structure with substantial vertical shear and horizontal variability. Myrup et al. found a substantial subsidence on the order of  $5 \text{ cm s}^{-1}$  over the Sacramento area during the study days by analyzing surface convergence and divergence patterns, suggesting that subsidence must be taken into account in air-quality studies in this area.

Zaremba and Carroll (1999) examined summer wind flow regimes over the Sacramento Valley using observations from surface meteorological sites from 1 May through 30 September 1991. Using conditional sampling, they determined the frequency of occurrence of three dominant summer wind regimes. Wind roses for the three wind regimes were produced for each station, and mean streamlines were constructed. These analyses provided a detailed climatological description of surface wind for the Sacramento Valley.

Although these previous studies helped to advance the knowledge of near-surface wind patterns and, to some degree, surface temperature evolution in central California, they provided little information about wind patterns above the surface, atmospheric stratification, evolution of the boundary layer, and the relationship between low-level winds and mesoscale thermal forcing. Our understanding to date about the boundary layer flow and temperature structure and evolution in central California has been based primarily on limited observations from twice-daily standard soundings at a few sites in the region. Because of the complex topography and coastline in the region, local and regional flows are expected to vary significantly across central California and to contribute substantially to large spatial and temporal variations in pollutant distributions.

In June–September of 2000, as part of the Central California Ozone Study (CCOS; Fujita et al. 1999; information available online at <http://www.arb.ca.gov/airways/CCOS/CCOS.htm>), a network of 22 915-MHz radar wind profilers/radio acoustic sounding systems (RASS) was deployed to central California, with the highest density in the Central Valley. This dense network provided continuous measurements of hourly wind

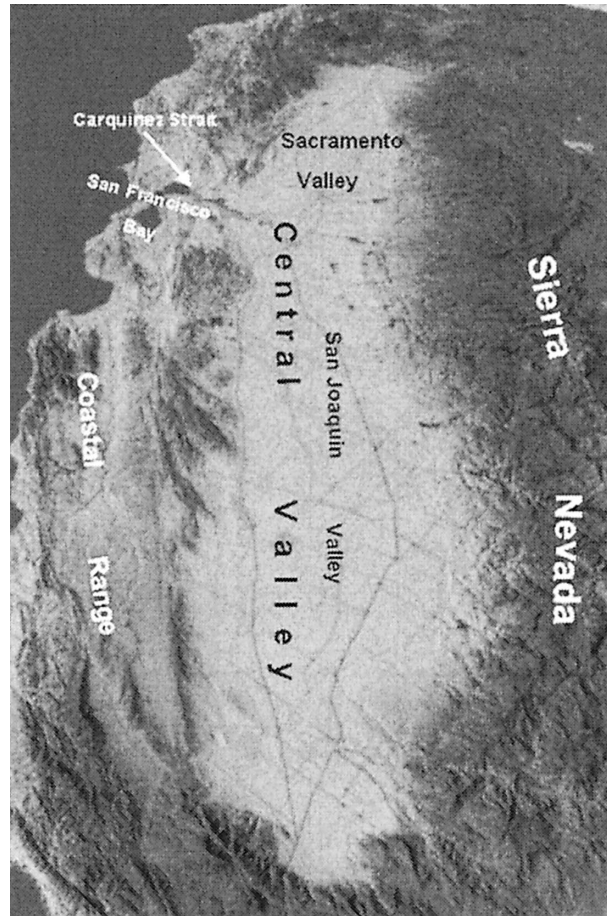


FIG. 1. Central California topography.

profiles in the lowest 2 km and virtual temperature profiles in the lowest 1 km at a vertical resolution of approximately 100 m, producing a dataset that is unprecedented in temporal, vertical, and horizontal resolution. In this paper, we present detailed analyses of this dataset to gain an improved understanding of the complex three-dimensional flow structures, their time variation, and their relationship to local and mesoscale thermal forcing.

## 2. Topography and summer climate in central California

The dominant feature of central California topography is the approximately 600-km-long Central Valley, which is bounded on the east by the Sierra Nevada and on the west by the Coast Ranges (Fig. 1). The Coast Ranges parallel the coastline, with peaks over 1.3 km above mean sea level (MSL), while the Sierra Nevada reaches altitudes from 2 to over 3 km. The Cascade Mountains bound the valley to the north, while the Tehachapi Mountains separate the Central Valley from the Mojave Desert to the south. The “Central Valley” is

actually composed of two valleys: the Sacramento Valley, which covers the northern third, and the San Joaquin Valley, which covers the southern part of the Central Valley. The two valleys merge in the delta region east of San Francisco where the Sacramento and San Joaquin Rivers flow together and then turn westward to flow through the Carquinez Strait—a gap in the Coast Ranges—into San Francisco Bay and the Pacific Ocean. The delta region is near or slightly below sea level, and the valley floor slopes slightly upward to about 160 m MSL at the northern end of the Sacramento Valley and about 200 m MSL at the southern end of the San Joaquin Valley. There are a number of prominent canyons issuing from both the Coast Ranges and the Sierra Nevada, but the floors of both the Sacramento and San Joaquin Valleys are flat, without any prominent terrain features except for the isolated Sutter Butte (645 m MSL) in the northern part of the Sacramento Valley.

In summer, the climate of central California is governed by the semipermanent Pacific high, which keeps storm tracks far to the north of California. Large-scale subsidence from this high pressure center often produces clear skies and an elevated subsidence inversion that extends over the entire region. Because the synoptic-scale flows are usually weak, the primary flows in the region are produced by differential heating between water and land and between the valley and surrounding mountain ranges. According to previous studies (Schultz et al. 1961; Frenzel 1962; Hays et al. 1984; Moore et al. 1987; Zaremba and Carroll 1999), the prevailing summertime wind pattern is dominated by marine air that penetrates through the Carquinez Strait, moves through the delta region, and splits into two currents flowing north and south into the Sacramento and San Joaquin Valleys, respectively. Superimposed on this dominant flow pattern are diurnally varying, thermally driven local circulations that flow up the mountain slopes during the day and down the slopes at night.

### 3. The dataset and the methods of analysis

The wind profiler/RASS network was operated by the National Oceanic and Atmospheric Administration (NOAA) Environmental Technology Laboratory. Information on the network and data from the CCOS study can be found online (<http://www.etl.noaa.gov/programs/modeling/CCOS/data>). The locations of the profiler/RASS instruments used in the current analyses are shown in Fig. 2, and the site information, including station names, three-digit identifiers, elevations, and latitudes and longitudes, is summarized in Table 1. Most of the sites were located within the Central Valley, with only a few outside the valley. The majority of the sites collected data for the entire 4-month CCOS experimental period from the beginning of June through the end of September of 2000, but several sites began data collection in July and, therefore, had somewhat shorter data records. A number of profilers reported data gaps in the

4-month-long time series, but the gaps were generally short, and no sites suffered from extensive periods of missing data. A real-time quality-control algorithm (Merritt 1995) was used at the profiler sites to remove spurious radar signals from migrating birds, which are known to affect radar profiler wind data (Wilczak et al. 1995). In addition, we removed additional suspicious data by using quality-control checks based on both signal-to-noise ratio and the requirement of neighborhood continuity at any given hour and temporal continuity at any given site.

To compare profiler data that were reported at somewhat different range-gate heights and to facilitate the computation of mean vertical profiles when range gates changed during the observational period, hourly profiles of wind and temperature at each site were first interpolated to a regular vertical grid above the ground at 100-m intervals. Then, at each vertical level, mean temperature and horizontal wind components for each hour of the day were obtained by averaging data for that particular hour for the entire observation period. The typical number of observations that went into the average for each hour ranged from 80 to 110; this number decreased rapidly above 1500 m for wind and above 800 m for temperature, above which heights more missing data were reported because of the well-known decrease of signal-to-noise ratios with elevation. Time-height cross sections of mean wind and temperature were constructed for each site. At each site, hodographs of mean winds were also constructed for each height to show both wind speed and direction at each of the 24 hours of the day. The resulting hodographs are presented in the standard way: the vector wind at a given hour is determined by drawing a vector from the coordinate origin (indicated by a plus sign) to the hourly data point for the time of interest. Every sixth data point [at 0000, 0600, 1200, and 1800 Pacific standard time (PST)] is labeled on the hodograph. A zero wind speed at a particular hour of the day can be produced by either calm winds at that hour for every day, or, more likely, by light winds with no preferred direction.

The consistency of the winds from day to day at a given time of day (the *wind consistency*; Stewart et al. 2002) was computed as the ratio of the vector mean wind speed to scalar mean wind speed at that time, such that

$$C_j^n = \frac{\sqrt{\bar{u}^2 + \bar{v}^2}}{\bar{S}} = \frac{\sqrt{\left(\frac{1}{N} \sum_{i=1}^N u_i\right)^2 + \left(\frac{1}{N} \sum_{i=1}^N v_i\right)^2}}{\frac{1}{N} \sum_{i=1}^N \sqrt{u_i^2 + v_i^2}}, \quad (1)$$

where  $C_j^n$  denotes wind consistency at the  $j$ th hour of the day at the  $n$ th site in the profiler network and  $\bar{S}$  is the mean wind speed. Because the vector mean speed is always smaller than or equal to the scalar mean wind speed,  $C_j^n$  values fall between 1 and 0, with 1 indicating

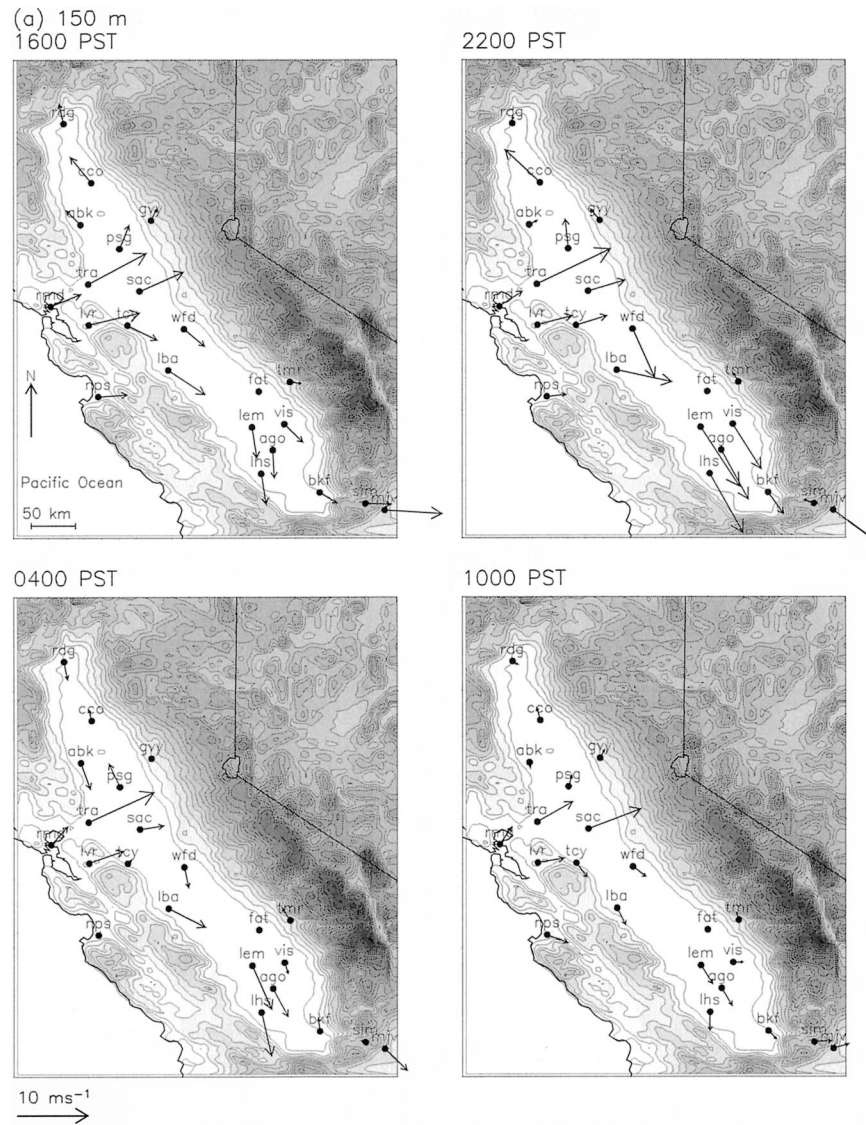


FIG. 2. Mean horizontal wind vectors at (a) 150, (b) 450, and (c) 1050 m AGL at 1600, 2200, 0400, and 1000 PST.

that the wind blows from the same direction at a given hour every day and 0 implying that wind is equally likely from all directions or that it blows one-half of the time from one direction and one-half of the time from the opposite direction. A larger  $C_j^n$  value usually indicates more consistent wind direction, provided that the sampling time period is sufficiently long.

In addition to the data from the profiler/RASS network, hourly surface observations from 13 locations in the area for the 4-month CCOS period were also analyzed. The 13 sites, all of which are standard U.S. Surface Airways Observation stations, have hourly measurements of sea level and station pressures, temperature and dewpoint, relative humidity, cloud cover, cloud type, and descriptive weather. The site information for

these surface stations is summarized in Table 2, and the site locations can be found in Fig. 3. Further information on the surface observations can be obtained from the National Climatic Data Center, where the data are archived. A direct comparison of the profiler/RASS observations with the surface observations allows us to determine to what degree the spatial and temporal variations of wind and temperature patterns revealed by the conventional surface network represent the patterns at higher elevations in the boundary layer. Understanding the representativeness of surface observations has practical significance because intensive observations from a dense profiler/RASS network are very costly, whereas surface observations are available routinely at low cost.

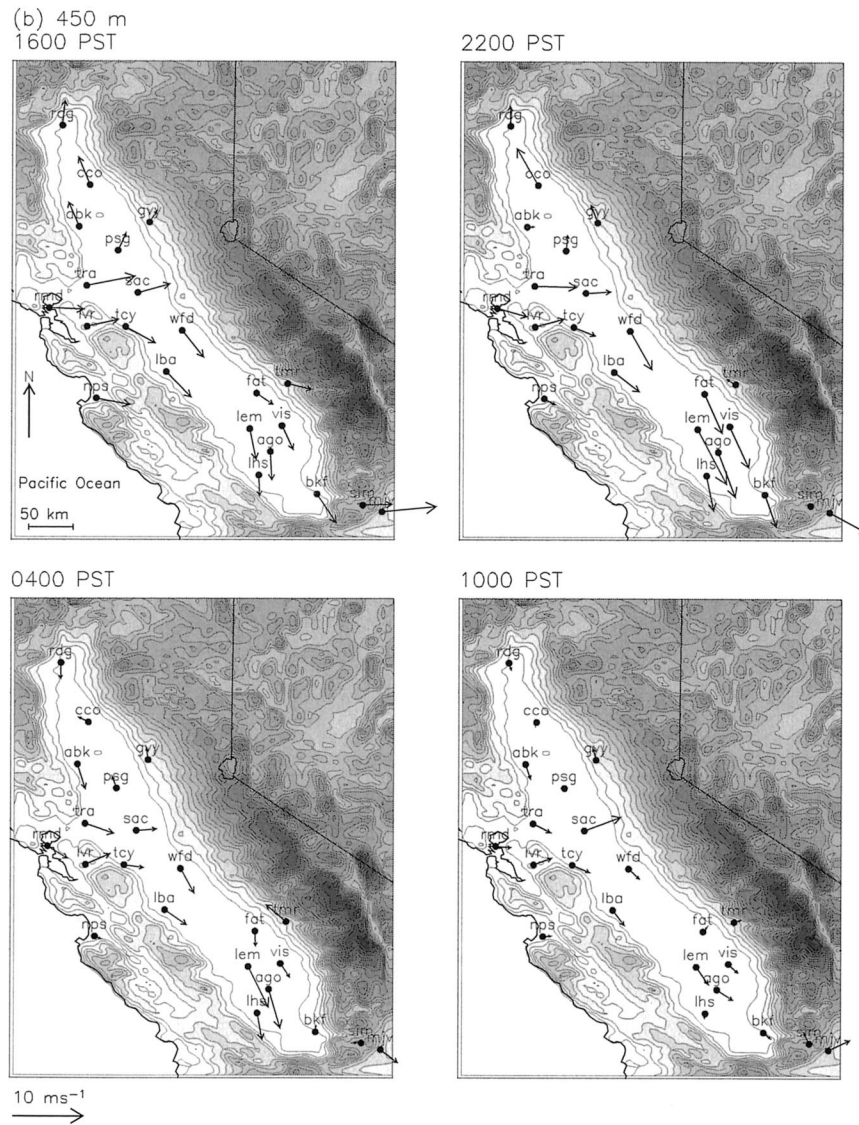


FIG. 2. (Continued)

**4. Results**

*a. Horizontal wind patterns and their diurnal variations*

The mean horizontal wind field patterns and their diurnal evolution are shown in Fig. 2 for four representative times (1600, 2200, 0400, and 1000 PST) at three levels above ground (150, 450, and 1050 m AGL). The wind profilers in the greater San Francisco Bay area [Richmond (rmd), Travis Air Force Base (AFB; tra) and Livermore (lvr)] experience westerly flows all day (Fig. 2a). Despite the weak diurnal variations in wind direction at these sites, wind speeds exhibit a distinct diurnal variation, with higher speeds in late afternoon and early night and lower speeds in the morning hours. The influence of topography is clearly evident. Higher terrain

to the north and south of Travis Air Force Base located at the edge of the Sacramento Valley produces a channeling effect that enhances the westerly onshore flow passing through the site, producing a mean wind speed greater than 10 m s<sup>-1</sup> during most of the day. At Livermore, located in the Livermore Valley in the eastern bay area, winds are almost parallel to the local valley axis.

The westerly onshore flows, after entering the Central Valley, split into two branches. One branch flows northward into the Sacramento Valley, and the other flows southward into the San Joaquin Valley. The mean wind speeds and directions differ considerably among the stations in the Sacramento Valley. At Sacramento (sac) winds are persistently from the west and southwest at speeds of up to 10 m s<sup>-1</sup>. Farther up valley, southeast-

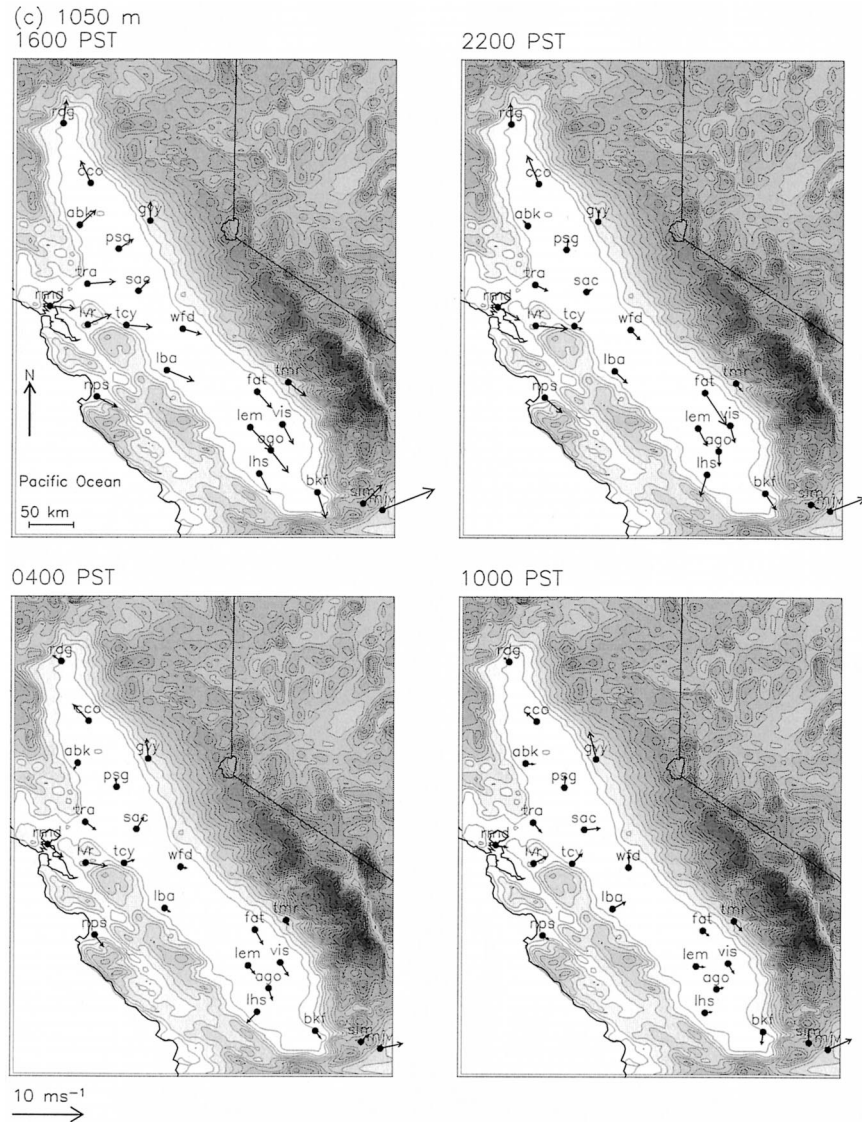


FIG. 2. (Continued)

erly up-valley winds are found at all sites during the daytime. At night, the up-valley winds at Redding (rdg) and Abuckle (abk) shift to down valley (i.e., from the north-northwest), but at Chico (cco) and Pleasant Grove (psg), winds remain up valley even at night, although speeds are considerably lower than during the daytime.

In the San Joaquin Valley, mean winds are predominantly from the northwest but with a pronounced diurnal variation of wind speed. At several sites in the southern San Joaquin Valley, the mean northwesterly winds exceed  $10 \text{ m s}^{-1}$  at night, becoming much weaker during the daytime. At Visalia (vis), a westerly wind component develops following sunrise, an indication of the development of upslope flows. A small southerly wind component occurs at Bakersfield (bkf) between midnight and early morning, representing a local down-slope flow at this southernmost site in the valley.

The mean horizontal wind patterns in Fig. 2a reveal areas of horizontal convergence and divergence in the Central Valley. Because winds are predominantly up valley, convergence occurs at both the northern and southern ends of the valley, where up-valley flows are blocked by the high mountains. This effect is clearly seen by the changes of wind speed and direction between Chico and Redding and between Angiola (ago) and Bakersfield. The convergence of horizontal wind at these locations is stronger at night (2200 and 0400 PST plots) than during the day (1000 and 1600 PST plots). Diffuence occurs in the flow bifurcation zone of the delta region as the strong incoming westerly flow splits to flow northward up the Sacramento Valley and southward up the San Joaquin Valley.

Except for a small decrease in wind speed, the 450-m-level mean horizontal wind patterns and their time

TABLE 1. Wind profiler site and data information.

Name	Identifier	Lat ( $^{\circ}$ N)	Lon ( $^{\circ}$ E)	Alt (m MSL)	No. of days of data
Arbuckle	abk	39.10	-122.04	33	122
Angiola	ago	35.95	-119.54	60	122
Bakersfield	bkf	35.35	-118.96	120	122
Chico	cco	39.69	-121.91	41	113
Fresno	fat	36.77	-119.71	100	113
Grass Valley	gvy	39.17	-121.11	689	122
Los Banos	lba	37.07	-120.87	35	122
Lemoore	lem	36.27	-119.80	67	122
Lost Hills	lhs	35.62	-119.69	80	122
Livermore	lvr	37.70	-121.90	65	83
Mojave	mjv	35.09	-118.15	850	122
Monterey	nps	36.69	-121.76	51	122
Pleasant Grove	psg	38.77	-121.52	10	122
Redding	rdg	40.52	-122.30	154	122
Richmond	rmd	37.95	-122.40	111	122
Sacramento	sac	38.18	-121.25	6	122
Simi Valley	sim	34.30	-118.80	283	65
Tracy	tcy	37.70	-121.40	60	83
Trimmer	tmr	36.90	-119.30	520	122
Travis AFB	tra	38.27	-121.92	17	122
Visalia	vis	36.31	-119.39	81	122
Waterford	wfd	37.65	-120.67	60	97

variations (Fig. 2b) closely resemble those at lower levels (Fig. 2a). Veering of winds with height occurs at Richmond and Travis Air Force Base, with winds at 450 m turning clockwise in relation to those at the 150-m level. Travis Air Force Base experiences the largest wind speed decrease with height, with the speed at 450 m being less than one-half of that at the 150-m level. At 1050 m AGL (Fig. 2c), mean winds are significantly weaker across the entire network, which is mainly a result of averaging winds of variable directions. The general pattern and diurnal variation remain, to some degree, unchanged.

Many of the features in the horizontal wind fields in the boundary layer as revealed by the wind profiler network are consistent with the behavior of near-surface winds that are routinely observed by surface meteorological

stations in the area. Figure 3 shows horizontal wind vectors at 17 surface stations, as averaged over the same time period as the radar profiler data. The surface winds exhibit similar spatial and temporal variations as those found at nearby profiler locations in Fig. 2a. A significant difference is that wind speeds at the surface stations are substantially lower, which is particularly evident at Sacramento and Lemoore (lem).

Detailed time variations of mean vector winds at individual stations can be seen best in hodographs, which are shown in Fig. 4 for selected profiler sites. The 24-h wind hodographs reveal how both wind speed and direction change during the course of the day, including the direction of rotation of winds during the diurnal cycle and the time of the day during which maximum and minimum wind speeds occur. In a comparison of

TABLE 2. Surface observational sites.

Name	Identifier	Lat ( $^{\circ}$ N)	Lon ( $^{\circ}$ E)	Alt (m MSL)
Bakersfield	bkf	35.43	-119.03	149
Blue Canyon	bcy	39.27	-120.70	1605
Bishop Airport	bis	37.36	-118.35	1250
Concord	con	37.99	-122.05	5
Fresno	fat	36.77	-119.71	100
Hayward Executive Airport	hwd	37.65	-122.10	13
Lemoore	lem	36.33	-119.95	67
Livermore	lvr	37.70	-121.82	120
Modesto	mod	37.62	-120.95	22
Napa County	nap	38.20	-122.28	5
Redding	rdg	40.52	-122.30	154
Red Bluff	rdb	40.15	-122.25	108
Sacramento	sac	38.18	-121.48	6
Santa Rosa	sra	38.50	-122.80	35
San Jose	sjs	37.37	-121.92	15
San Francisco	sfo	37.61	-122.40	3
Stockton	sto	37.88	-121.22	8

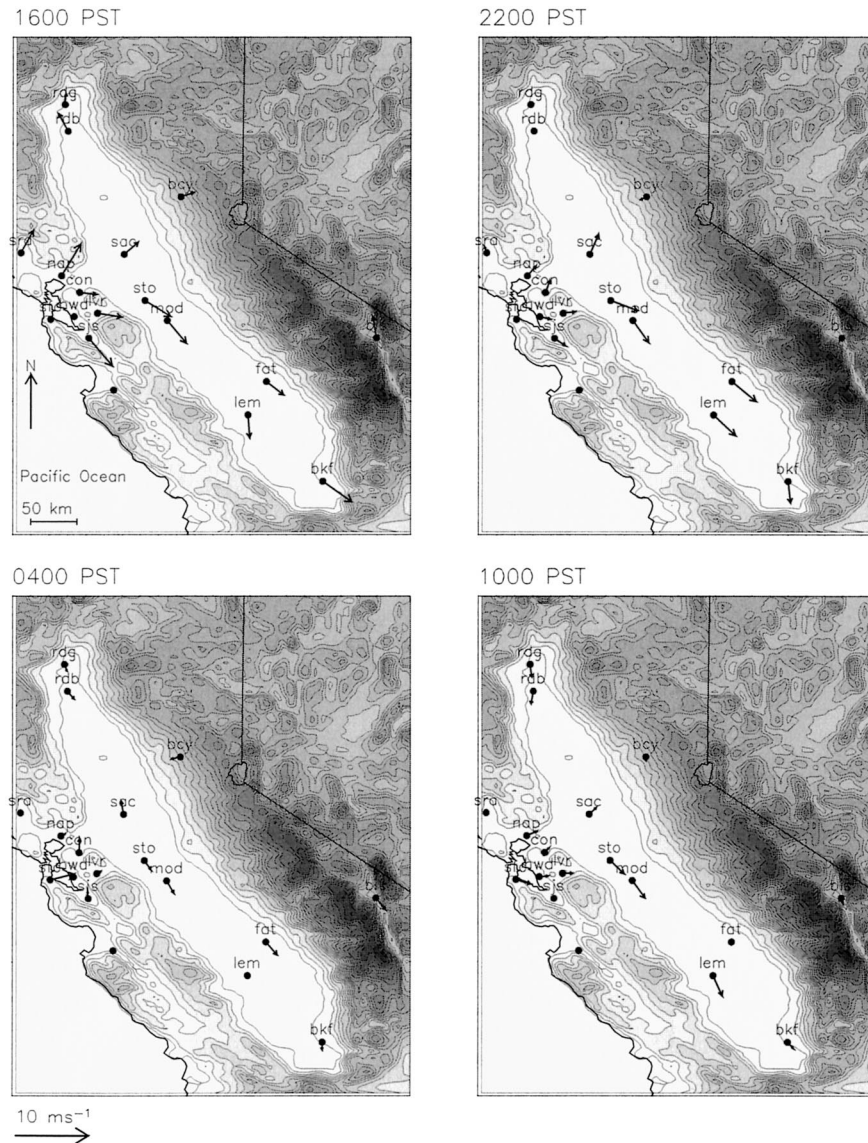


FIG. 3. Mean horizontal wind vector at the surface using observations from the surface network. The wind vector scale and times are as in Fig. 2.

hodographs from different locations, those over the wider parts of the valley floor [e.g., Water Ford (wfd) and Pleasant Grove] tend to assume a more circular shape than those in areas with more confined topography (e.g., rdg). The wind rotations are counterclockwise at some stations (psg, lvr, and sac) and are clockwise at others (wfd, vis, and bkt). At several sites (rdg, ago, and lem), the rotation changes direction during the course of the day. At the northernmost site in the Sacramento Valley (rdg), where the valley becomes very narrow, winds are bidirectional, with the transition to down valley and downslope occurring around midnight and the transition to up valley and upslope occurring around noon. The maximum up-valley/upslope wind occurs around sunset (between 1800 and 1900 PST), and the downslope wind

peaks around sunrise (0600 PST). Bidirectional winds are also observed at Trimmer (tmr) near the exit of King's Canyon, where northwesterly up-canyon winds peak at 1900 PST and weaker southeasterly down-canyon flows reach a maximum around 0600 PST. The hodographs at the sites in the southern San Joaquin Valley (lem, ago, and vis) reveal a rapid acceleration of northwesterly up-valley winds in the evening, with peak wind speeds of generally greater than  $10 \text{ m s}^{-1}$  occurring 1–2 h before midnight. The daytime wind speeds are substantially lower at these locations, and a minimum speed is usually reached in the morning hours.

Comparisons of hodographs of profiler winds with hodographs of nearby surface winds (Fig. 5) reveal some differences in the diurnal evolution of mean winds at



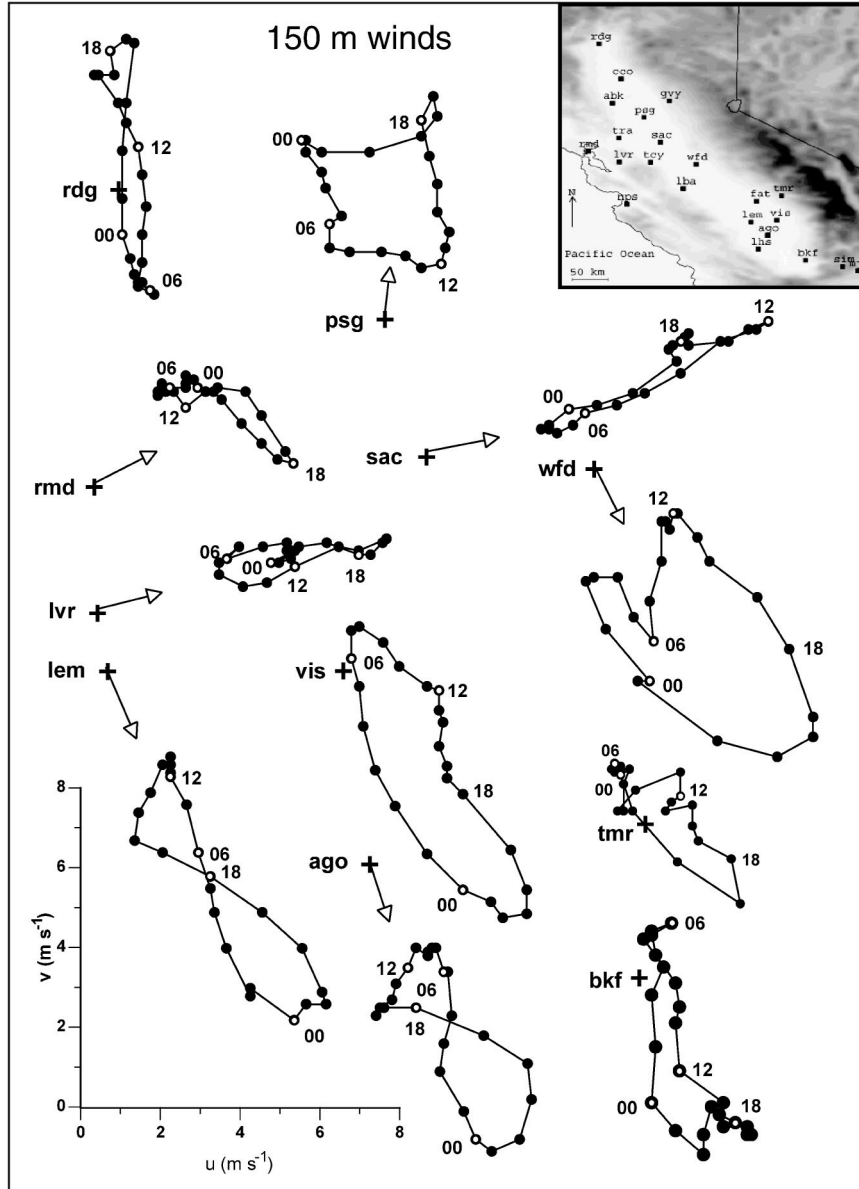


FIG. 4. Mean wind hodographs at 150 m AGL for selected sites in the Central Valley, with locations indicated in the map in the upper-right corner of the figure. The mean winds for each site for each hour of the period of record can be obtained by drawing a vector from the coordinate origin (plus sign labeled with site identification) to the black dots on the corresponding curve. On some hodographs a short arrow is included to point out the general direction from the coordinate origin to the corresponding curve. There is a point on the curve for each of the hours of the day; 0000, 0600, 1200, and 1800 PST (white dots) are labeled. The axis in the lower left of the figure should be moved to the individual coordinate origins to obtain quantitative  $u$  and  $v$  wind velocity components for a given site.

the surface and those in the boundary layer above the surface. Although the wind vector rotation and wind speed variation with time are, in general, similar between the near-surface winds and those in the boundary layer, there are usually some differences in the timing of maximum and minimum wind speeds during the diurnal cycle. The largest difference occurs at Sacramento, where the maximum wind speed is found around 1800

PST near the surface but around noon at 150 m AGL. At Livermore, winds are from the west at the surface and shift to the west-southwest aloft. At Redding, the near-surface wind direction is more confined to the north-south direction, possibly because the valley terrain is narrower near the surface. The differences are relatively small at sites in the southern San Joaquin Valley.

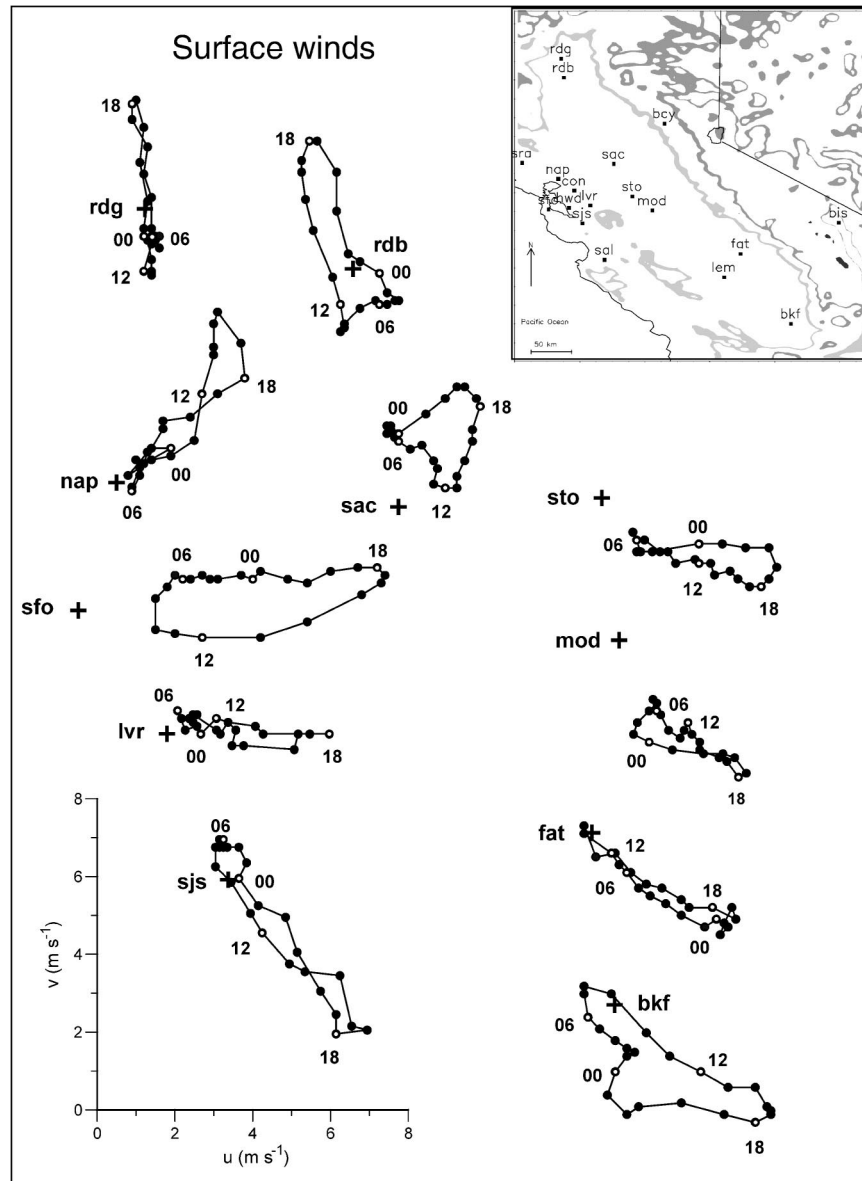


FIG. 5. Same as in Fig. 4 but for surface winds.

### b. Vertical wind structure and its evolution

Comparisons of horizontal winds at three different heights in Fig. 2 have shown significant variations of both wind speed and direction with height above ground. To understand the detailed vertical variation of horizontal winds, the time–height cross sections of mean vector winds are shown in Fig. 6 for selected stations in the San Joaquin Valley (Fig. 6a), the Sacramento Valley (Fig. 6b), and outside the Central Valley (Fig. 6c). Overlaid on the mean wind vectors in Fig. 6 are contours of wind consistency as computed using Eq. (1) to indicate the variability of the winds that were composited to compute the mean wind vectors.

The majority of stations in the San Joaquin Valley (Fig. 6a) show a similar pattern in the vertical structure of horizontal wind during the diurnal cycle. The northwesterly flows that are dominant during the nighttime occupy the lowest 800 m. This layer of northwesterly winds is characterized by a low-level wind maximum occurring below 300 m and a sharp decrease of speed above the maximum. This low-level jetlike structure is particularly pronounced at Lemoore and Angiola, where a peak speed of over  $10 \text{ m s}^{-1}$  is found at 300 m and where the wind speeds drop to below  $2 \text{ m s}^{-1}$  by 1000 m. Only the mean winds are shown here; the peak wind at these sites on individual days can be even stron-

ger. The very high values of wind consistency ( $>0.8$ ) indicate the high day-to-day consistency of the low-level wind maximum in this part of the valley during the summer season. Above 1000 m, the consistency values drop to 0.2–0.4 and the mean wind speeds are low, indicating the highly variable nature of winds aloft. At Trimmer, located next to the exit of King's Canyon, the observations show a well-developed southeasterly down-canyon flow at night and early morning and a northwesterly up-canyon flow from late morning until late evening. The down-canyon flow layer is approximately 500–600 m deep, somewhat shallower than the daytime up-canyon flow layer, which extends to 800 m above the surface. The vertical profiles of wind speed clearly reveal the jetlike down-canyon flow, with an elevated maximum approximately 500 m above the surface. This phenomenon is consistent with other observations of valley exit jets (Whiteman 2000; Fast and Darby 2004).

Unlike in the San Joaquin Valley, where the horizontal winds are relatively homogeneous, have similar vertical structure at different sites, and evolve similarly with time, the Sacramento Valley winds (Fig. 6b) exhibit vertical variations that are very different from one location to another. In the lower Sacramento Valley at Pleasant Grove, predominant up-valley winds from the southeast are confined to the lowest 500–600 m, with maximum wind speeds of 4–7  $\text{m s}^{-1}$  below 300 m. Farther up the valley at Chico, different structures are observed in which well-developed south-southeasterly winds extend to over 1 km during most of the day, except for the morning period during which winds are weak and disorganized. At the northernmost end of the valley (Redding), southerly up-valley flows in the afternoon extend to over 1 km, and both wind speed and direction in the southerly flow layer are relatively uniform with height. Downslope or down-valley flows start to develop in the late evening as winds at the lowest level shift to a northerly direction. These northerly winds continue to grow in depth throughout the rest of the night, reaching 800 m between 0800 and 1000 PST. The northerly winds gradually veer to a southerly direction above 1300 m, an indication, perhaps, of return flow. Of interest is that mean winds at Arbuckle show many similarities to those at Redding, although the two stations are relatively far apart. A core of relatively strong northerly winds that is over 500 m deep develops at night and in the early morning at Arbuckle but is absent at Pleasant Grove and Chico. It is not clear from the observations what the driving forces are for the north-northwesterly winds at Arbuckle. A plausible explanation is that they may represent a thermally driven downslope flow from the slopes to the west and northwest of the Arbuckle site. Numerical simulations with well-resolved topography can help to confirm this speculation. At Sacramento in the delta region, the prevailing westerly winds occupy the lowest 500–600 m. The high wind speeds in the lowest 300 m fall off rapidly with

height. Winds aloft shift to a southerly direction with mean speeds much lower than those below.

In the bay area west of the Central Valley (Fig. 6c), westerly onshore flows that are relatively uniform with height exceed 1 km in depth at Richmond. Significant diurnal variations in wind speed are not limited to the lowest levels, but occur throughout the entire boundary layer. Wind speeds and directions and their time variations in the mid- and upper boundary layer at Travis Air Force Base are similar to those over Richmond, but westerly onshore flows in the lower levels are much stronger at Travis Air Force Base than at Richmond. The depths of the enhanced westerly flow layer correspond well to terrain height to the north and south of Travis Air Force Base, indicating the strong influence of terrain channeling on the low-level flow.

The wind consistency values are generally low (0.2–0.4) at elevations between 1000 and 2000 m AGL (where wind directions vary from day to day). In the lowest 1000 m, where winds are dominated by thermally driven or topographically forced flows, the winds are much more consistent, with wind consistencies exceeding 0.6 or even 0.9 at many locations and during most of the day, except for brief transitional periods. Low consistency values in the lower boundary layer are almost exclusively associated with the wind direction change during the morning or evening transitions at sites that are influenced strongly by terrain. For example, at Redding and Arbuckle, a consistency value below 0.1 occurs around midnight and around noon when the transitions between upslope/up-valley and downslope/down-valley winds occur. In a similar way, at Trimmer and Simi Valley (sim), the lower consistency values also correspond well to the reversal of wind direction, which occurs somewhat earlier than at Redding. Changes in synoptic conditions and the sunrise/sunset time during the 4-month period are likely to smear the transition times and contribute to lower consistency values.

The vector wind profiles shown in Figs. 6a, 6b, and 6c reveal several interesting features about the vertical wind structure and its diurnal variation. The first feature is a general decrease of wind speed with height. Although the low mean wind speeds in the upper boundary layer are partially a result of averaging winds of variable directions, an inspection of profiler wind observations on each day confirms that wind speeds, in general, are lower in the upper boundary layer than in the lower boundary layer. Because of the earth's frictional effect, winds in the lower atmosphere normally increase with distance from the surface. Figure 6 shows that over central California mean winds in the summer season generally decrease with height in the 1- to 2-km-deep atmospheric boundary layer during daytime. This feature can be attributed to a combined influence of the weak summertime synoptic forcing associated with persistent anticyclonic weather patterns over the region and strong near-surface thermal forcing associated with the ocean–land temperature contrasts and the diabatic heat-

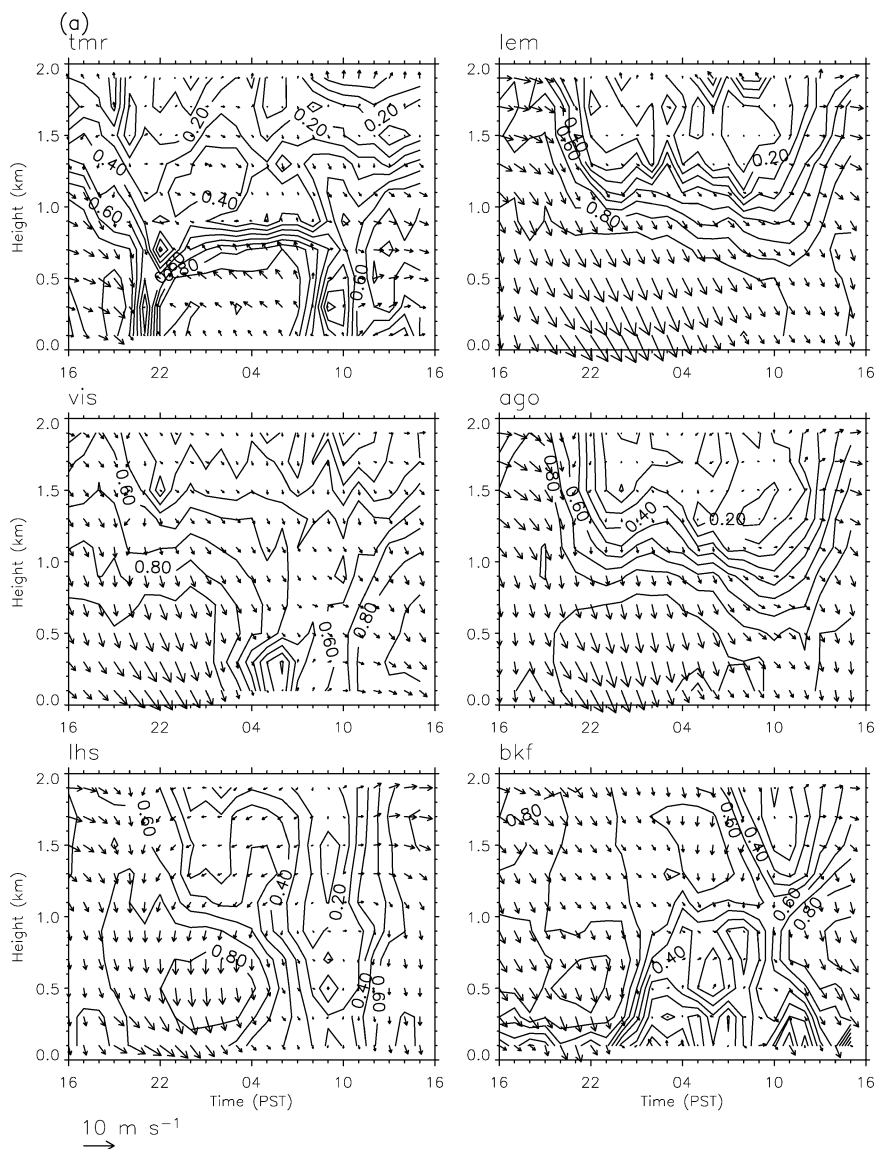


FIG. 6. Time-height cross sections of mean wind vectors for selected stations in the (a) San Joaquin and (b) Sacramento Valleys and (c) outside the Central Valley. The contours are persistence values calculated using Eq. (1).

ing and cooling of mountain slopes. This pattern of reversed vertical wind shear is clearly evident at almost all of the sites. At many locations, the lowest wind speeds occur at 1000–1500 m AGL and during the time period from early morning to noon. Another striking feature that is revealed by the wind profiler data for the first time at many locations in the Central Valley is how deep the mesoscale thermally induced or topographically forced flows are in the area. For example, the nighttime down-valley winds at Redding and Arbuckle are over 500 m deep, with even deeper daytime counterparts. The prevailing northwesterly up-valley flows in the San Joaquin Valley also exceed 600 m during many hours of the day.

### c. The vertical temperature structure

The RASS measures virtual temperature, but because of the low humidity in the region, the difference between virtual temperature and temperature should generally be within 1°C. We will, therefore, neglect their difference in our discussions below. Because at higher range gates the RASS measurements usually have low signal-to-noise ratio and the data are known to be unreliable, we will limit our discussion of the RASS temperature profiles to the lowest 600 m above ground.

The vertical temperature structure and its evolution are summarized from RASS observations at eight selected locations in Fig. 7. The afternoon boundary layers

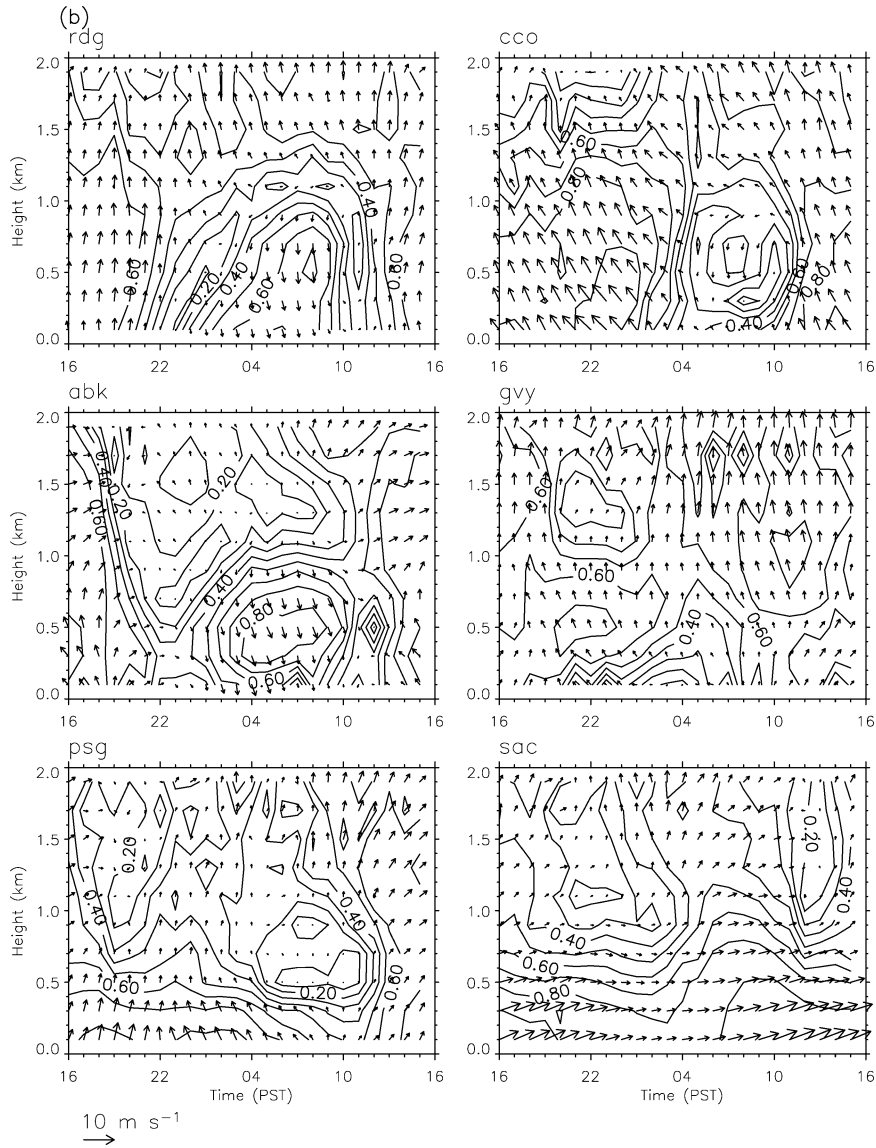


FIG. 6. (Continued)

in the Central Valley are characterized by mixed layers with a temperature lapse rate near the dry adiabatic lapse rate, and the heights of the mixed layers exceed 800–1000 m. In contrast, at the coastal area (e.g., Richmond) the boundary layer temperature structure is near isothermal, even during the daytime, indicating a stable stratification. Shortly after sunset, a temperature inversion begins to develop at the coast and in the delta region and inversion strength increases during the night to reach vertical gradients near  $0.01^{\circ}\text{C m}^{-1}$ , or  $1^{\circ}\text{C (100 m)}^{-1}$ . Away from the delta in the mid- to upper Sacramento and San Joaquin Valleys, a temperature inversion does not form until late at night, with the evening and early nighttime temperatures being generally isothermal. The boundary layer at night is more stable in

the San Joaquin Valley, with temperature inversions, than it is in the Sacramento Valley, where the temperature structure is isothermal. It is interesting to note that at the northern end of the Sacramento Valley (Redding), temperatures continue to decrease with height even at night, although nighttime lapse rates are much smaller than the moist adiabatic lapse rate. The less stable atmosphere at Redding as compared with other parts of the valley may be attributed to the narrower terrain at that location, which promotes cross-valley flows and turbulent mixing, as has been suggested from observations made in narrow canyons (Whiteman et al. 1999). In a similar way, at Bakersfield, in the southern end of the San Joaquin Valley, the vertical temperature structure remains isothermal rather than increasing with

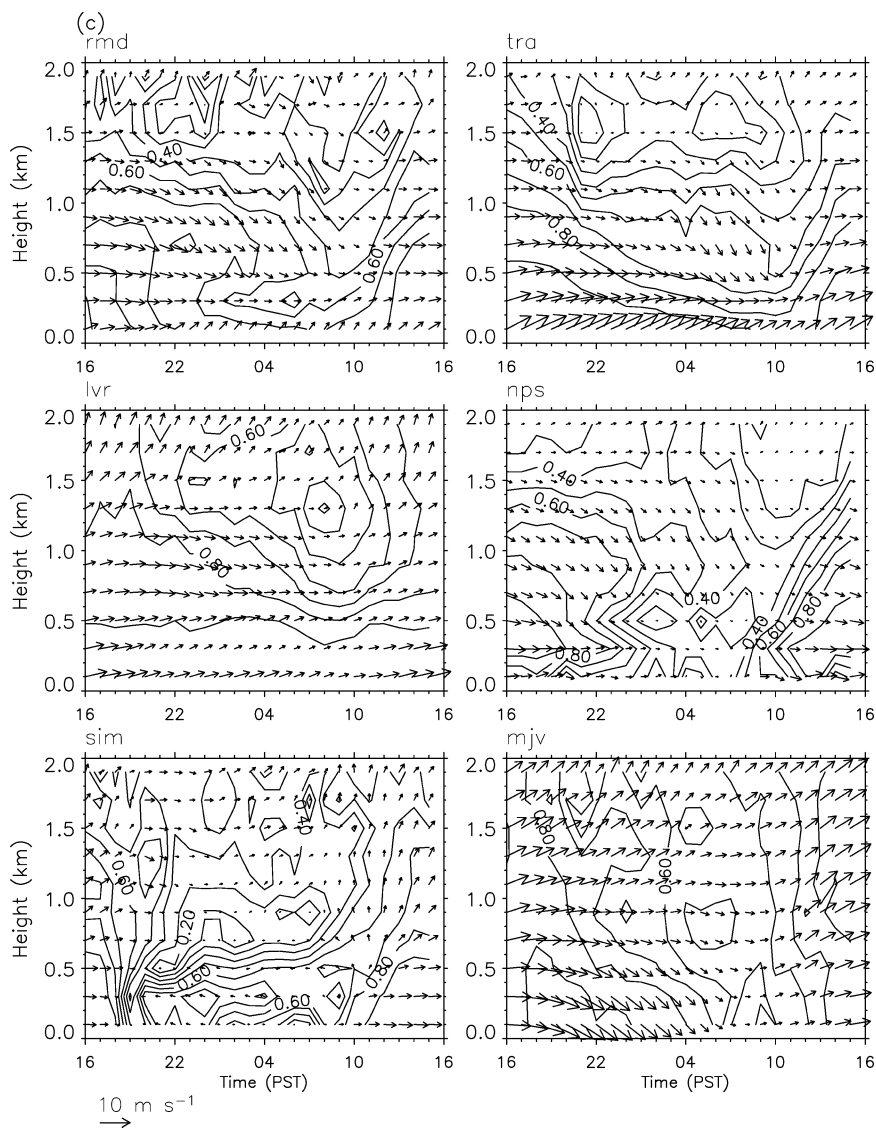


FIG. 6. (Continued)

height as at stations north of Bakersfield (e.g., ago and lem), suggesting that the boundary layer is less stable at this site as compared with other sites in the southern San Joaquin Valley.

A comparison of temperature profiles at the sites in Fig. 7 at a given time clearly indicates a large along-valley variation of temperature structure. This along-valley temperature gradient in the boundary layer can be viewed more clearly in Fig. 8, which shows temperature contours as a function of height and distance from Sacramento at four times of day (1600, 2200, 0400, and 1000 PST). The plot is constructed using data from selected profiler/RASS sites that were located on the valley floor not far from the valley centerline. Data from these sites were projected perpendicularly onto the valley centerline. Throughout the diurnal cycle and in the

lowest 600–800 m of the atmosphere, the lowest temperatures on the along-valley cross section are always found in the delta region, due primarily to the constant intrusion of cool ocean air through the Carquinez Strait. The boundary layer temperatures increase consistently with distance away from the delta region, and the increase is slightly more rapid toward the south in the San Joaquin Valley than toward the north in the Sacramento Valley. At any given time and at all levels, the highest temperatures are always found near the north and south ends of the Central Valley, with the maximum value at the southern end being 1°–2°C higher than at the northern end. The upward tilt of the temperature contours toward both ends during the day also indicates that mixed-layer heights resulting from the heating of the valley floor and sidewalls increase with up-valley

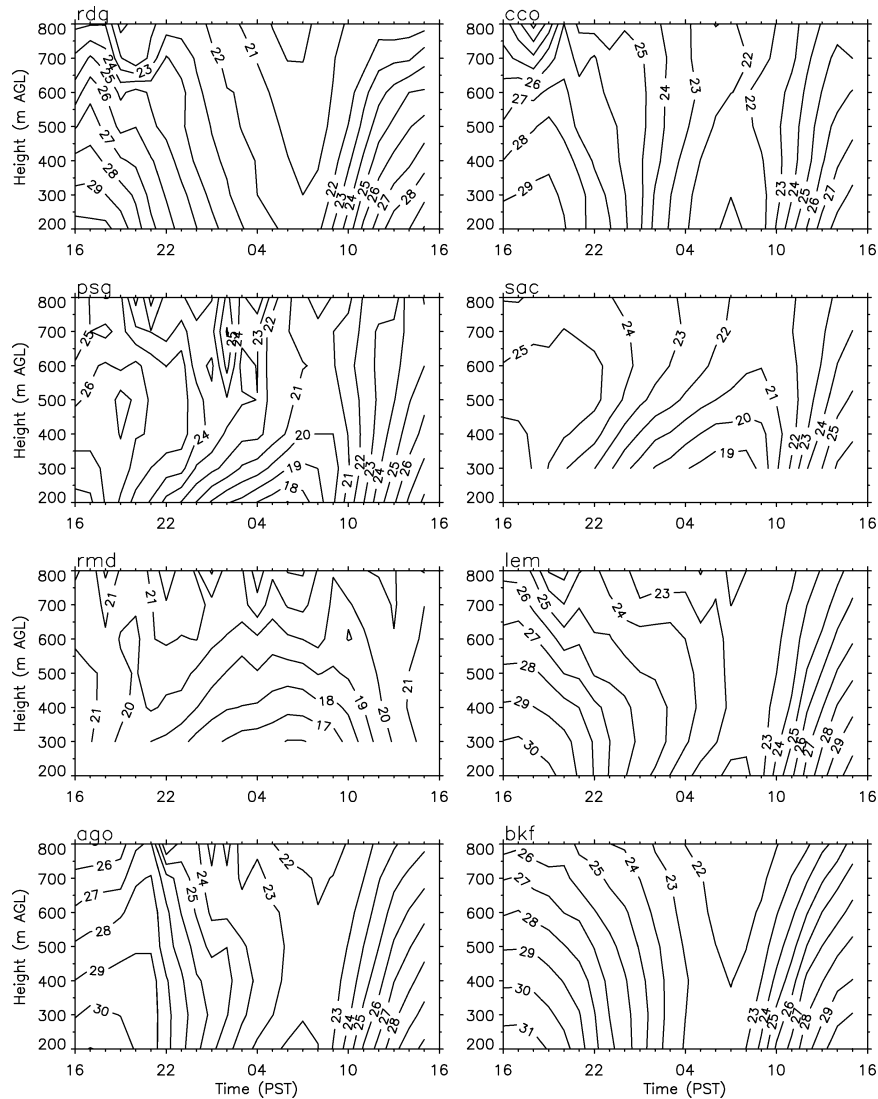


FIG. 7. Time-height cross sections of temperatures ( $^{\circ}\text{C}$ ) at selected locations.

distance. Although the limited height range of the RASS data prohibits an evaluation of the mean mixed-layer depths, the afternoon mixed layers appear to be higher than 1000 m except in the delta region where a mixed layer, if it develops, is likely to be only a few hundred meters deep.

*d. Mesoscale thermal forcing and wind speed oscillations*

Wind observations from the surface and profiler networks reveal a summertime low-level flow pattern in the region that is strongly influenced by land-ocean thermal contrasts and by diabatic heating and cooling of the mountain slopes. Because the area has only a single upper-air sounding site at Oakland, which is outside the Central Valley, previous studies have relied on

surface temperature and pressure observations to provide an explanation for the complex behavior of thermally driven flows in the Central Valley. Frenzel (1962), for example, examined diurnal variations of pressure differences between selected surface stations. He found that the observed changes in near-surface westerly wind speeds at Travis Air Force Base appear to be in good agreement with the pressure difference variations between San Francisco and Sacramento, but the winds in the northern and southern parts of the Central Valley do not seem to be in phase with the along-valley pressure gradient oscillations. The wind profiler/RASS network makes it possible, for the first time, to examine the thermal forcing in the boundary layer above the surface and its role in determining the spatial and temporal wind variations in the region.

Figure 9 shows the diurnal variations of near-surface

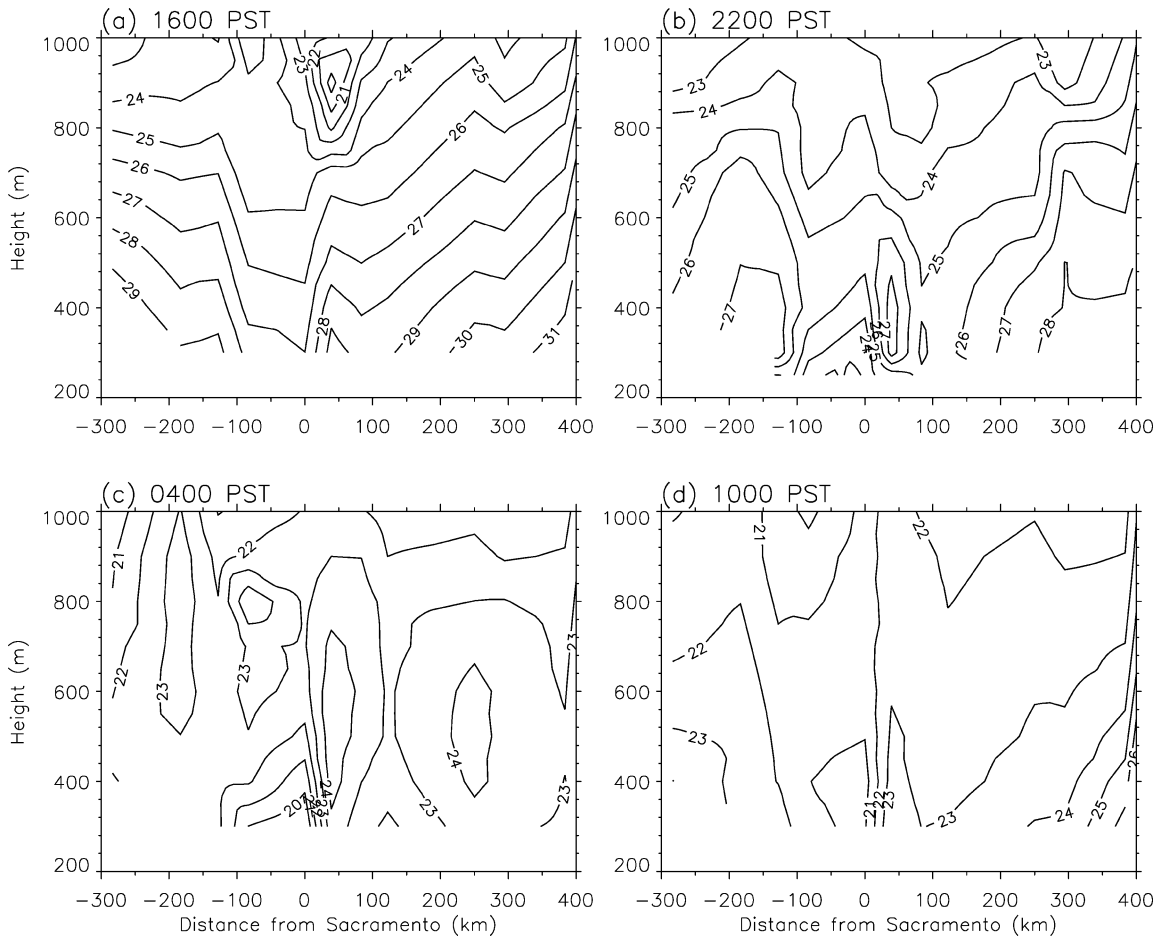


FIG. 8. Vertical cross sections of temperature ( $^{\circ}\text{C}$ ) along the centerline of the Central Valley from north to south for (a) 1600, (b) 2200, (c) 0400, and (d) 1000 PST.

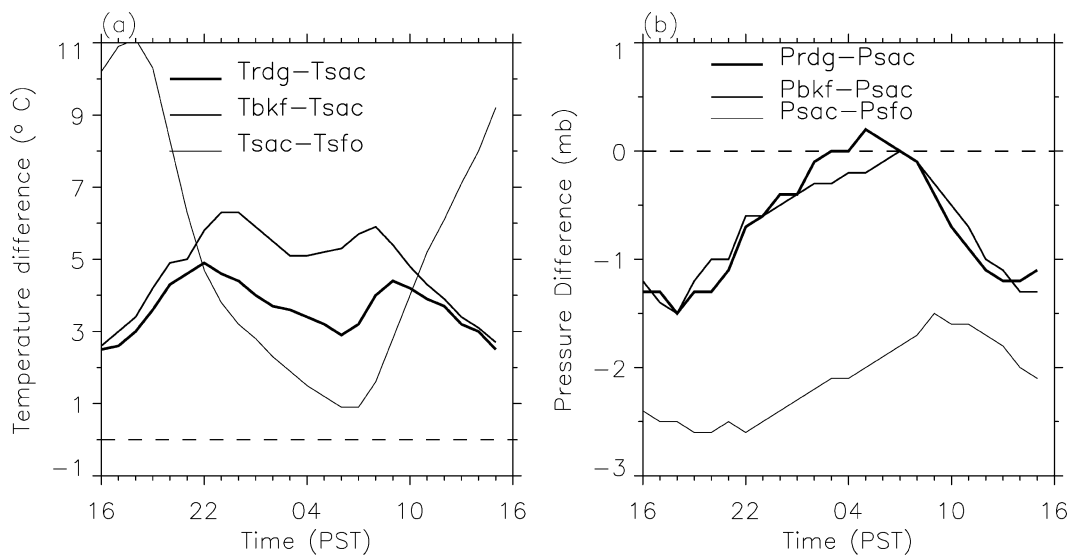


FIG. 9. Surface (a) temperature and (b) pressure differences between Sacramento and three stations: San Francisco, Redding, and Bakersfield.



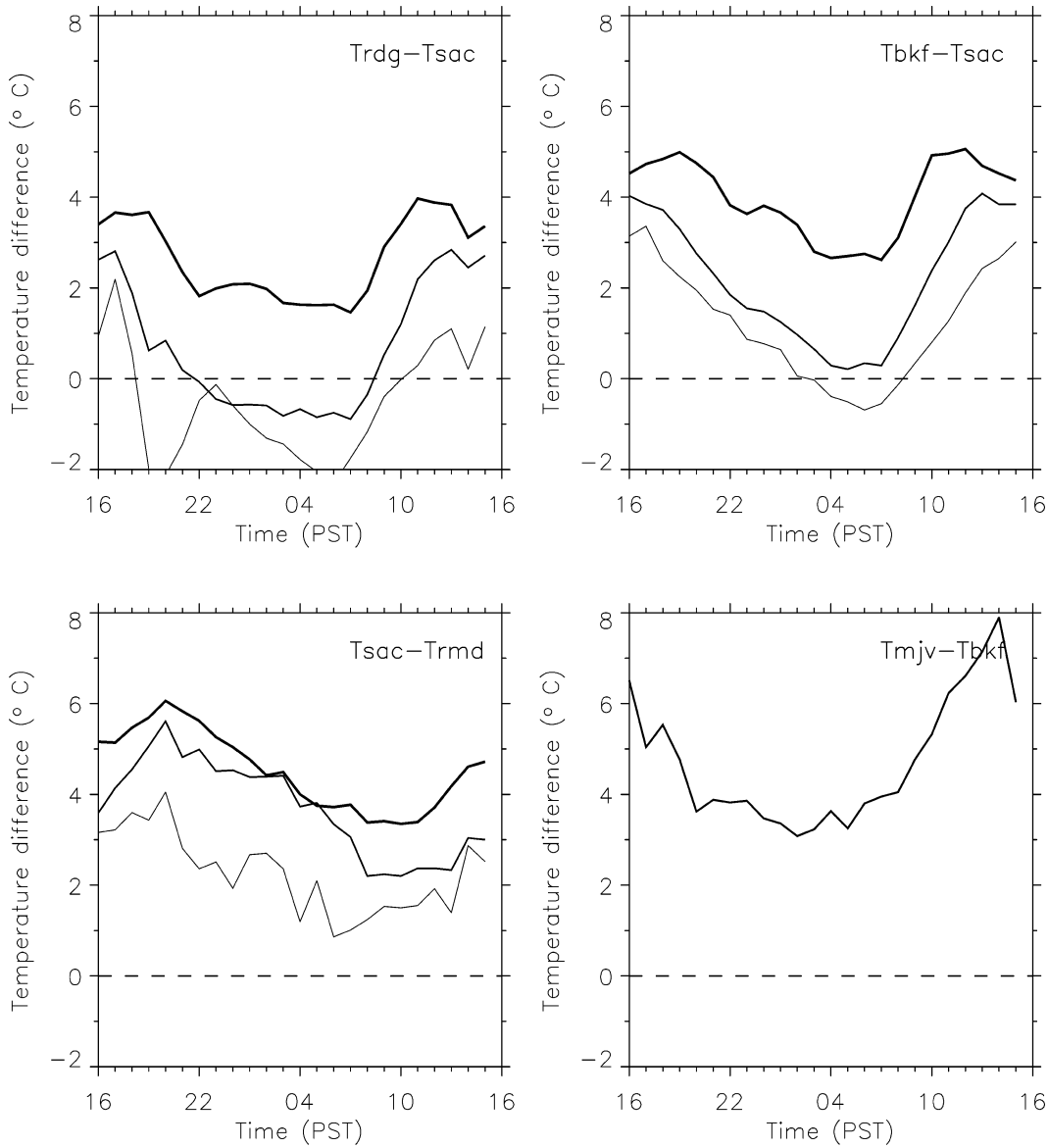


FIG. 10. Horizontal surface temperature differences between Sacramento and three stations: Redding, Bakersfield, and Richmond and between Bakersfield and Mojave at 200 (thick line), 600 (medium-thick line), and 800 (thin line) MSL.

temperature and sea level pressure differences between Sacramento and three other sites: San Francisco, Redding, and Bakersfield. These stations are selected to represent best the temperature and pressure gradients between the coast and the Central Valley (Sacramento – San Francisco), and along the valley axis in the Sacramento (Sacramento – Redding) and San Joaquin (Sacramento – Bakersfield) Valleys, respectively. The temperature and pressure differences were averaged over the entire 4 months from June through September of 2000. Figure 10 shows similar time series of temperature differences computed using RASS observations at three heights (200, 600, and 800 m) above mean sea level. Because there was no profiler/RASS at San

Francisco, the RASS observations at Richmond are used together with those at Sacramento to compute the coast-inland temperature gradients.

From Fig. 9, the temperature at San Francisco (or Richmond) is consistently lower than at Sacramento and the pressure is consistently higher; neither gradient reverses between day and night. The temperature difference exhibits a strong diurnal oscillation with a maximum amplitude of greater than 10°C occurring in late afternoon and a minimum of less than 2°C in the morning. The amplitudes of these temperature oscillations decrease rapidly with height (Fig. 10). The pressure gradient oscillation (Fig. 9) lags the temperature gradient oscillation by 1–2 h. The strong diurnal oscillation of

coastal-to-inland temperature and pressure gradients appears to be in phase with the diurnal variation of the westerly onshore flows observed by the profilers and surface stations in the bay area and in the delta region where observed winds usually reach maximum speeds in late afternoon and minimum speeds in the morning.

The temperature and pressure differences between the lower and upper Sacramento Valley (Sacramento and Redding) and the lower and upper San Joaquin Valley (Sacramento and Bakersfield) are much smaller than those between the coast and the interior valley (Fig. 9). The differences are always positive, with higher temperatures at Redding or Bakersfield than at Sacramento throughout the diurnal period. This along-valley thermal forcing directed in the up-valley direction is consistent with the low-level winds in the two valleys, which blow persistently up the valleys. The temperature and pressure difference oscillations in the two valleys closely track each other over the course of the day with slightly larger amplitude oscillations between Sacramento and Bakersfield than between Sacramento and Redding. Although weak, the temperature difference oscillation shows double peaks, one in late evening to midnight and the other in the morning, with a minimum value in early morning. The diurnal pressure difference oscillation, however, exhibits a sinusoidal pattern, with a single peak (maximum absolute value) in the late afternoon near sunset and a minimum (minimum absolute value) in early morning, and there is hardly any difference in the pressure gradient oscillation between the two valleys. Unlike the strong correlation found between the timing of maximum onshore winds and the timing of the peak coastal-inland pressure gradient force, the diurnal variation of the along-valley pressure gradient appears to be out of phase with the diurnal oscillation of along-valley winds, with the peak wind speed considerably lagging behind the peak pressure gradient.

Based on the studies of wind regimes in the Inn Valley in Austria, by Nickus and Vergeiner (1984) and Vergeiner and Dreiseitl (1987), an estimate of the response time of valley winds to pressure gradient forcing can be obtained using the following simplified equation of motion for the along-valley wind component:

$$\frac{\partial u}{\partial t} = -\frac{1}{\rho} \frac{\partial p}{\partial s} - \kappa u, \quad (2)$$

where advection and the Coriolis force are neglected,  $-\rho^{-1}(\partial p/\partial s)$  is the along-valley pressure gradient force, and  $-\kappa u$  represents friction, with  $\kappa$  being the linear friction coefficient. Using pressure data at Sacramento and Bakersfield and wind observations at sites between the two stations, we obtain an estimate for  $\kappa$  of  $7 \times 10^{-5} \text{ s}^{-1}$ . The relaxation or reaction time of the wind to switching the pressure gradient force on or off would be  $\tau = 1/\kappa \approx 1/(7 \times 10^{-5}) = 14\,286 \text{ s} \approx 4 \text{ h}$ . The hodographs in Fig. 4 show that, at most stations in the

southern San Joaquin Valley, maximum winds occur 1–2 h before midnight, which is consistent with the above prediction. It is interesting to note that when similar calculations are carried out using the observed coastal-inland pressure gradients and westerly onshore winds, the estimated wind response time reduces to near 0.5 h, suggesting an almost immediate response, which is in agreement with the finding that the wind and pressure gradient oscillations at the coast are nearly in phase.

As shown in Fig. 9, even at night the mean temperatures at the surface and in the lower boundary layer remain higher in the valley than temperatures over the coastal region, and the pressure gradient force between the coast and the interior valley dominates the along-valley pressure gradients at all times. On a larger scale, the temperature offshore is generally much colder than the temperature inland. The baroclinicity associated with the coastal-interior and ocean-land pressure differences is expected to result, through the thermal wind relationship, in a stronger north-northwesterly wind in the lower atmosphere than that aloft, where synoptic forcing dominates. This situation can be explained mathematically by the thermal wind relationship

$$\begin{aligned} \frac{\partial u_g}{\partial z} &\approx -\frac{g}{fT} \frac{\partial T}{\partial y} \quad \text{and} \\ \frac{\partial v_g}{\partial z} &\approx \frac{g}{fT} \frac{\partial T}{\partial x}, \end{aligned} \quad (3)$$

where  $u_g$  and  $v_g$  are geostrophic wind components and  $f$  is the Coriolis parameter. Because, according to the temperature observations from the surface and RASS network,  $\partial T/\partial y < 0$  and  $\partial T/\partial x > 0$ , Eq. (3) indicates that  $\partial u_g/\partial z > 0$  and  $\partial v_g/\partial z > 0$ , or

$$\begin{aligned} \Delta u_g &\approx -\frac{g}{f\bar{T}} \frac{\partial T}{\partial y} \Delta z > 0 \quad \text{and} \\ \Delta v_g &\approx \frac{g}{f\bar{T}} \frac{\partial T}{\partial x} \Delta z > 0, \end{aligned} \quad (4)$$

where  $\bar{T}$  is the mean temperature in the layer  $\Delta z$ . For north-northwesterly geostrophic winds,  $u_g > 0$  and  $v_g < 0$ , a combination that, according to Eq. (4), implies that the east-west geostrophic wind component  $u_g$  would increase with increasing height while the north-south component  $v_g$  would decrease with increasing height ( $v_g$  should be smaller in value or less negative). Because winds in the San Joaquin Valley are north-northwesterly with a north-south component that is much larger than the east-west component, Eq. (4) implies a decrease in the total geostrophic wind speed with increasing height. Using the RASS observations, we can estimate the mean temperature gradient in the lowest 600 m as  $\partial T/\partial x \approx -3 \times 10^{-5} \text{ C m}^{-1}$  and  $\partial T/\partial y \approx -1 \times 10^{-5} \text{ C m}^{-1}$ . At latitude  $36.5^\circ \text{N}$  (in the southern part of the San Joaquin Valley), the Coriolis parameter  $f \approx 8.65 \times 10^{-5} \text{ s}^{-1}$ . With the assumption that temperature averaged in the lowest 600 m is  $\bar{T} \approx 25^\circ \text{C}$ , Eq. (2)

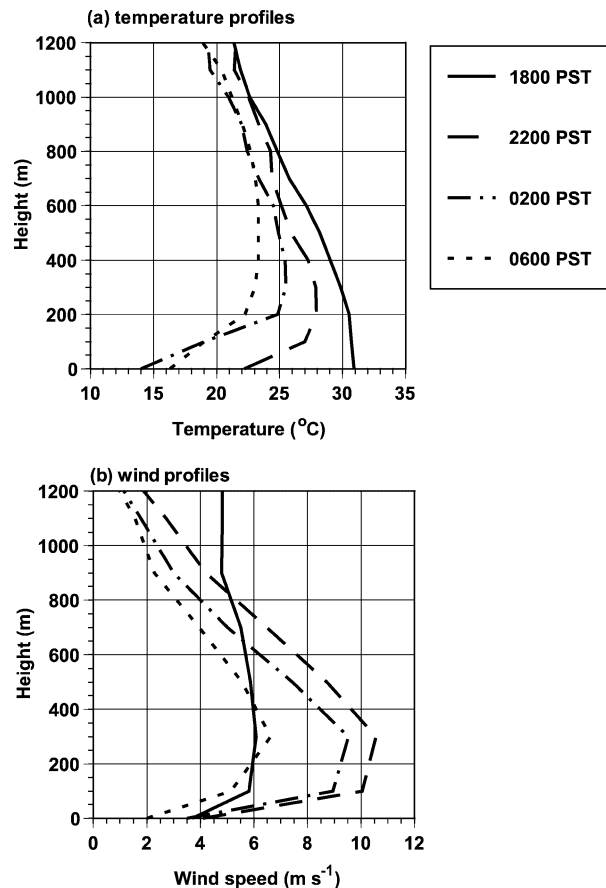


FIG. 11. Mean (a) temperature and (b) wind speed profiles at Lemoore at four different times of day.

yields a rate of wind speed decrease with height of approximately  $1 \text{ m s}^{-1} (100 \text{ m})^{-1}$ . This estimated value of vertical wind shear appears to match the observed vertical shear associated with the low-level wind maximum at stations in the southern part of the San Joaquin Valley very well. In the Sacramento Valley, winds are south-southeasterly with  $v_g > 0$ ,  $u_g < 0$ , and  $|v_g| \gg |u_g|$ , which, according to Eq. (4), implies an increase of geostrophic wind speed with height. This condition, which is unfavorable for the formation of a low-level wind maximum, is consistent with the absence of the observed low-level jet in the Sacramento Valley.

Figure 11 shows the observed vertical wind and temperature profiles at Lemoore for four times from evening to early morning. The profiles exhibit a classic behavior of low-level jets resulting from an inertial oscillation of winds above the surface-based inversion that decouples the layer above the inversion from surface friction (Blackadar 1957). As a radiation inversion began to grow upward from the surface after sunset, winds in the lowest several hundred meters accelerated from about  $6 \text{ m s}^{-1}$  to form a jet profile with maximum wind speed of over  $10 \text{ m s}^{-1}$  at about 300 m AGL. Above the maximum, speed decreases nearly linearly with height

at a rate close to  $1 \text{ m s}^{-1} (100 \text{ m})^{-1}$ . The maximum low-level jet speed occurred at 2200 PST, when the ageostrophic winds going through an inertial oscillation cycle are in the same direction as the prevailing north-northwesterly winds.

## 5. Discussion and conclusions

The availability of hourly wind and temperature profiles at 22 sites in central California during a 4-month period from June through September of 2000 has provided an unprecedented opportunity to extend our understanding of surface temperature and circulation patterns to the entire boundary layer for this region of great topographic complexity during the season of highest air pollution. The current study has examined horizontal wind patterns, the vertical wind structure and temporal variation, the boundary layer stratification and its evolution, and the relationship between the mesoscale thermal forcing and the boundary layer circulation.

The results and analyses in this paper are based on the mean wind and temperature values obtained using all the available data during the entire 4-month observational period. Similar analyses have been repeated with a subset of the data selected using the criterion that winds from the radar profilers at 1500 m MSL are less than  $5 \text{ m s}^{-1}$ . The purpose of the selection is to eliminate days on which synoptic winds are strong so as to better isolate thermally induced flows. The results from the analyses of the data subset, however, are very similar to those using all of the available data. An examination of synoptic conditions (i.e., periods of synoptic stagnation based on 850-hPa winds and daily precipitation) indicates that the summer of 2000 is typical climatologically for central California. We believe that the characteristics of the three-dimensional wind and temperature structure and evolution identified using the current dataset are representative of typical summer seasons for this region.

It has been known from surface observations that the summer-season climatological winds in the Central Valley of California are characterized by a split of westerly onshore flow that enters into the Central Valley in the delta region into two branches flowing northward into the Sacramento Valley and southward into the San Joaquin Valley, respectively. The profiler network revealed that this basic mean flow pattern, which is a result of mesoscale thermal forcing due to the land–ocean thermal contrast, is not confined to a shallow near-surface layer but rather extends upward to 800–1000 m. Although the flow pattern remains, wind speeds vary greatly with height, with a low-level wind maximum usually occurring in the lowest 300 m. At valley-floor sites away from sidewall slopes, the up-valley winds do not reverse direction during the course of the diurnal cycle; in the narrower part of the valley (e.g., near the northern and southern ends) or at sites close to the sidewalls, low-level winds reverse direction diurnally following the

slope diabatic heating and cooling cycle. Despite the persistency of the wind direction at most sites, wind speeds exhibit a strong diurnal variation throughout the boundary layer, with amplitudes decreasing with height.

The afternoon boundary layers in the Central Valley are characterized by mixed layers that are generally deeper than 1000 m AGL, and the mixed-layer heights increase with distance away from the delta region northward into the Sacramento Valley and southward into the San Joaquin Valley. Over the coast, however, the mean RASS temperature profiles show a near-isothermal structure even during the day, indicating that the mixed layer (if one develops at all) is very shallow. At night, a temperature inversion develops in the lowest 200–400 m of the valley, with near-isothermal layers aloft. Mean temperatures in the lowest 500 m are always warmer in the valley than at the coast and warmer in the upper valleys than in the lower valleys. The differences in temperatures produce pressure gradient forces both day and night that are directed inland from the coast and from the lower to upper valleys, although the magnitudes of the thermal forcing vary over the course of the day, with maximum values occurring in the late afternoon and minimum values in the early morning. The diurnal oscillation of the land–ocean or coast–inland thermal contrasts is in phase with the diurnal variations of westerly onshore winds. The diurnal oscillation of the prevailing along-valley flows, however, lags 4–5 h behind the oscillation in along-valley pressure gradient force, with the maximum along-valley winds occurring 1–2 h before midnight and the maximum pressure gradient occurring just before sunset. Well-defined low-level jets occur at sites in the southern San Joaquin Valley, with a maximum jet speed averaged over the summer season of more than  $10 \text{ m s}^{-1}$  at most sites and with a vertical wind shear of approximately  $0.01 \text{ s}^{-1}$  above the maximum. The height of the wind speed maximum is around 300 m above the surface, which is just above the top of the surface-based inversion as revealed by the RASS temperature profiles. The maximum jet speed occurs 1–2 h before midnight at which time the inertial oscillation of the ageostrophic winds comes into phase with the prevailing winds.

*Note added in proof.* It has come to our attention very recently that, during periods of dense nocturnal bird migration, the real-time wind profiler quality-control algorithm can fail to eliminate the bird contamination of the radar signal, as previously discussed by Merritt (1995). In addition, the simple neighborhood continuity check that we applied to the data in postprocessing will fail to remove contiguous bird-contaminated winds. For these reasons, an additional level of editing of profiler winds is commonly applied to 915-MHz wind profiler data, based either on an evaluation of the subhourly moments [signal-to-noise ratio (SNR), velocity, and spectral width] or on rapid changes in hourly SNR and wind velocities consistent with migration patterns. Al-

though data using a higher level of editing were available, they were not used in this analysis, leaving known periods of bird contamination in the dataset. Although we believe that the general findings presented in this article for daytime periods are unlikely to be altered by the possible contamination, the nighttime wind speeds will have been affected and, therefore, should be regarded with some caution. An assessment of the impact of the bird contamination on our results will be made in the near future.

*Acknowledgments.* We thank Dr. Saffet Tanrikulu from the San Francisco Bay Area Air Quality District, the California Air Resources Board, and the NOAA Environmental Technology Laboratory for making the radar wind profiler data available to us. We also thank Francis Ludwig at Stanford University and Chris Doran at Pacific Northwest National Laboratory for their careful reviews of early versions of this manuscript and three anonymous reviewers for their detailed, constructive review comments. This work was supported by the U.S. Department of Energy (DOE) under the auspices of the Atmospheric Sciences Program of the Office of Biological and Environmental Research under Contract DE-AC06-76RLO 1830 at Pacific Northwest National Laboratory (PNNL). PNNL is operated for DOE by Battelle Memorial Institute.

#### REFERENCES

- Blackadar, A. K., 1957: Boundary layer wind maxima and their significance for the growth of nocturnal inversions. *Bull. Amer. Meteor. Soc.*, **38**, 283–290.
- Fast, J. D., and L. S. Darby, 2004: An evaluation of mesoscale model predictions of down-valley and canyon flows and their consequences using Doppler lidar measurements during VTMX 2000. *J. Appl. Meteor.*, **43**, 420–436.
- Frenzel, C. W., 1962: Diurnal wind variations in central California. *J. Appl. Meteor.*, **1**, 405–412.
- Fujita, E., R. Keislar, W. Stockwell, H. Moonsmuller, D. DuBois, D. Koracin, and B. Zielinska, 1999: Central California Ozone Study. California Air Resources Board Tech. Rep., 90 pp.
- Hays, T. P., J. K. Kinney, and N. J. Wheeler, 1984: California surface wind climatology. California Air Resources Board Rep., 180 pp. [Available from California Air Resources Board, 2020 L Street, Sacramento, CA 95814.]
- Merritt, D. A., 1995: A statistical averaging method for wind profiler Doppler spectra. *J. Atmos. Oceanic Technol.*, **12**, 985–995.
- Moore, G. E., C. Daly, M.-K. Liu, and S.-J. Huang, 1987: Modeling of mountain–valley wind fields in the southern San Joaquin Valley, California. *J. Climate Appl. Meteor.*, **26**, 1230–1242.
- Myrup, L. O., D. L. Morgan, and R. L. Boomer, 1983: Summertime three-dimensional wind field above Sacramento, California. *J. Climate Appl. Meteor.*, **22**, 256–265.
- Nickus, U., and I. Vergeiner, 1984: The thermal structure of the Inn Valley atmosphere. *Arch. Meteor. Geophys. Bioklimatol. Ser. A*, **33**, 199–215.
- Schultz, H. B., N. B. Akesson, and W. E. Yates, 1961: The delayed ‘sea breezes’ in the Sacramento Valley and the resulting favorable conditions for application of pesticides. *Bull. Amer. Meteor. Soc.*, **42**, 679–687.

- Stewart, J. Q., C. D. Whiteman, W. J. Steenburgh, and X. Bian, 2002: A climatological study of thermally driven wind systems of the U.S. Intermountain West. *Bull. Amer. Meteor. Soc.*, **83**, 699–708.
- Vergeiner, I., and E. Dreiseitl, 1987: Valley winds and slope winds—Observations and elementary thoughts. *Meteor. Atmos. Phys.*, **36**, 264–286.
- Whiteman, C. D., 2000: *Mountain Meteorology—Fundamentals and Applications*. Oxford University Press, 355 pp.
- , S. Zhong, and X. Bian, 1999: Wintertime boundary layer structure in the Grand Canyon. *J. Appl. Meteor.*, **38**, 1084–1102.
- Wilczak, J. M., and Coauthors, 1995: Contamination of wind profiler data by migrating birds: Characteristics of corrupted data and potential solutions. *J. Atmos. Oceanic Technol.*, **12**, 449–467.
- Zaremba, L. L., and J. J. Carroll, 1999: Summer wind flow regimes over the Sacramento Valley. *J. Appl. Meteor.*, **38**, 1463–1473.